https://doi.org/10.15407/mineraljournal.45.04.003
UDC 549.08

O.M. Ponomarenko[1], DrSc (Geology), Academician of NAS of Ukraine, Director
E-mail: pan.igmof@gmail.com; https://orcid.org/0000-0002-5179-6091
L.M. Stepanyuk[1], DrSc (Geology), Corresp. Member of NAS of Ukraine, Prof., Deputy Director
E-mail: stepaniuk@nas.gov.ua; https://orcid.org/0000-0001-5591-5169
A.S. Smolyar[1], PhD (Technology of Silicates and Refractory Inorganic Materials), Senior Researcher
E-mail: smolyar@nas.gov.ua; https://orcid.org/0009-0002-2201-6823
A.O. Burkhan[1], PhD (Materials Science Engineering), Senior Researcher
E-mail: burkhan.anatoliy@ukr.net; https://orcid.org/0009-0002-3155-0171
O.M. Bloshchanevich[2], Researcher
E-mail: alex.bl337777@gmail.com; https://orcid.org/0009-0008-3624-9082
A.I. Stegniy[2], Researcher
E-mail: steg888999@gmail.com; https://orcid.org/0009-0007-4082-4425
V.L. Bekenev[2], Senior Researcher
E-mail: alitub@ukr.net; https://orcid.org/0009-0003-2438-4731
A.V. Stepanenko[1, 2], PhD (Solid State Physics), Senior Researcher
E-mail: stepart6913@gmail.com; https://orcid.org/0000-0003-2282-146X
V.G. Khomenko[3], DrSc (Engineering), Associate Professor
E-mail: v.khomenko@i.ua; https://orcid.org/0000-0003-0013-8010
M.P. Brodnikovskyy[2], PhD (Solid State Physics), Head of Department
E-mail: nbrodnik@gmail.com; https://orcid.org/0000-0001-7649-7373
B.S. Khomenko[4], Senior Engineer
E-mail: bskhomenko40@gmail.com; https://orcid.org/0009-0006-0707-7707
[1] M.P. Semenenko Institute of Geochemistry, Mineralogy and Ore Formation of the NAS of Ukraine
34, Akad. Palladin Ave., Kyiv, Ukraine, 03142
[2] I.M. Frantsevich Institute for Problems of Materials Science of the NAS of Ukraine
3, Omeliana Pritsaka Str., Kyiv, Ukraine, 03142
[3] Kyiv National University of Technologies and Design
Department of Chemical Technologies and Resource Saving
2, Mala Shyianovska Str., Kyiv, Ukraine, 01011
[4] V.I. Vernadsky Institute of General and Inorganic Chemistry of the NAS of Ukraine
32/34, Akad. Palladin Ave., Kyiv, Ukraine, 03142

ELECTRONIC STATES DENSITY, RESISTIVITY, AND PHASE COMPOSITION OF $CaTiO_3$ PEROVSKITE WITH ISOMORPHIC IMPURITY OF NIOBIUM

The application of materials with a perovskite structure has currently become one of the most promising approaches for the development of photovoltaic systems. A method for high-speed synthesis (under 15 minutes) of $CaTiO_3$ perovskite — TiO_2 rutile with the possibility of concurrent doping of the product has been developed. The density of electronic states,

C i t e: Ponomarenko, O.M., Stepanyuk, L.M., Smolyar, A.S., Burkhan, A.O., Bloshchanevich, O.M., Stegniy, A.I., Bekenev, V.L., Stepanenko, A.V., Khomenko, V.G., Brodnikovskyy, M.P. and Khomenko, B.S. (2023), Electronic States Density, Resistivity, and Phase Composition of $CaTiO_3$ Perovskite with Isomorphic Impurity of Niobium. *Mineral. Journ. (Ukraine)*, Vol. 45, No. 4, pp. 03-12. https://doi.org/10.15407/ mineraljournal.45.04.003

phase composition features, and resistivity of niobium-doped perovskite ($CaTiO_3$) were investigated. The calculations of the density of electronic states for niobium-doped $CaTiO_3$ have shown that at low concentrations of niobium, the samples exhibit conductivity characteristic of semiconductors. Since niobium has one more valence electron compared to titanium, as the niobium content increases, the Fermi level shifts to the band of free states. This shift of the Fermi level should lead to a change in the nature of the conductivity of doped crystals, eventually transitioning to metallic conductivity at high concentrations of niobium. Composite analysis ($CaTiO_3$ + TiO_2) by X-ray diffraction has shown that the use of niobium as a doping element significantly accelerates the $CaTiO_3$ synthesis reaction, and increases the perovskite concentration in the sample. The concentration of $CaTiO_3$ in the sample the with niobium is 83% vol. at a temperature of 900 °C and a synthesis time of 5 min, whereas when using a mixture without Nb, the content of perovskite will be only 58% vol. at a synthesis time of 12 min. X-ray phase analysis methods confirm the formation of a solid solution (doping) $Ca(Ti,Nb)O_3$, resulting in the preparation of samples ($CaTiO_3$ + TiO_2) with resistivity inherent to semiconductors.

Keywords: *perovskite, synthesis, XRD, solid solution, doping, semiconductors, conductivity.*

Introduction. The energy crisis is the most challenging problem that humanity has faced, because energy consumption [6] grows annually and reached 574 EJ in 2017, with an estimated increase to more than 1100 EJ by 2050. The burning of fossil fuels for electricity and heat generation has significantly changed the Earth's atmosphere due to high levels of CO_2 emissions, contributing to the greenhouse effect and climate imbalance. Renewable energy technologies have to be developed as alternatives to fossil fuels and nuclear energy. These include solar, wind, hydropower, geothermal, and tidal energy. Thus, the annual potential for solar power generation on Earth is estimated [4] to be 1575—49837 EJ, depending on the region of the world, which significantly exceeds the annual global energy consumption of 574 EJ. Photovoltaic systems are currently the fastest growing energy generation technology, constituting 1.7% of the current energy generation.

One of the most interesting new approaches in the development of photovoltaic systems has become the application of perovskite structure compounds. The optimization of perovskite-based devices has led to an increase in energy conversion efficiency from 3% to more than 22% in just 9 years. Due to their high photovoltaic performance, use of affordable materials, and cost-effective manufacturing processes, perovskite solar cells are anticipated to be competitive with crystalline silicon units.

Calcium titanate ($CaTiO_3$) belongs to the group of perovskites having an orthorhombic crystal structure at room temperature, transitioning into a tetragonal and cubic crystal structure within the temperature range of 1200—1700 °C [31, 8]. It finds utility as a dielectric or ferroelectric material in radio engineering and electronic industries [10, 27]. Article [24] mentions that $CaTiO_3$ is also used for immobilization of radioactive waste. At low temperatures, it exhibits ferroelectric properties and is used in electroluminescent devices and sensors [24, 3]. Due to perovskite activeness in UV light radiation, its high photocorrosion and heat resistance [24, 12, 35] were studied regarding its potential use as a photocatalyst for manufacturing of solar cells.

Various methods are used to obtain $CaTiO_3$. Initially, the synthesis of $CaTiO_3$ was carried out using a solid-phase reaction [32] (at relatively high temperatures, 900—1400 °C) from TiO_2 and $CaCO_3$. In an effort to reduce reaction temperatures, shorten process times, and achieve improved properties of $CaTiO_3$-based materials due to nanosized particles, wet chemical methods, such as hydrothermal synthesis [35], co-deposition method [34], microwave hydrothermal synthesis [20], sol-gel method [33] have been used for synthesis. The application of these methods has led to the development of materials with complex shapes and structures, exhibiting different physical, chemical and mechanical properties. The main advantage of most of these wet chemical methods is that $CaTiO_3$ is obtained at relatively low temperatures (600—900 °C).

The most modern representation of the ideal perovskite structure (Fig. 1) is given in studies [21, 22]. This structure comprises a framework of TiO_6 octahedral that are interconnected by shared vertices. Ti^{4+} are located at the nodes of a primitive cubic cell, at the center of which Ca^{2+} is positioned with a coordination number of 12.

The aim of this study was to develop a high-speed method for the relatively low-temperature

synthesis of the composite ($CaTiO_3$ + TiO_2) with semiconductor properties, which according to the results from several studies [5, 19, 17], exhibits advantages when compared with pure $CaTiO_3$. This method makes it possible to obtain $CaTiO_3$ at temperatures ranging from 700 to 900 °C and within a synthesis time of 2—5 min. Additionally, we studied some features of niobium-doped $CaTiO_3$.

Initial materials. To obtain the ($CaTiO_3$ + + TiO_2) composite in the laboratory, PTM-1 grade titanium powder and calcium hydroxide supplied by OUEEN COLOR were utilized. For doping, niobium powder from the MbP brand, supplied by Grand Lada, was used. In prospect, we plan to develop a high-performance industrial process.

The results of the study, conducted using the fluorescent X-ray diffraction method to determine the elemental composition of the initial powders, indicated that they correspond to the relevant standards: Ti — TU 14-22-57-92; $Ca(OH)_2$ — GOST 9179-2018; Nb — GOST 26252-84.

Research methods and equipment. The authors developed [29, 25, 28] and manufactured split and one-piece furnace designs. The synthesis was carried out using the metallothermic method in an air environment. The powder mixture in the melting pot was loaded into a furnace heated to the appropriate temperature, held for 3—12 minutes, and then abruptly unloaded.

The study of perovskite powders by X-ray diffraction was carried out on a DRON-3M diffractometer using Cu-Kα radiation. The diffraction patterns were taken by point shooting with a step of 0.05° and exposure time of 5 s; the sampling interval was 20—70°. To conduct a qualitative phase analysis, the Analyze software package with PDF-2 database was used. Quantitative X-ray phase studies were carried out with the Rietveld method using the Powder cell software package. At the first stage, theoretical crystal lattices were developed for each of the phases contained in the powder. At the second stage, the superpositions of these theoretical lattices were compared to experimental — diffractograms using the least squares method. The results of this comparison were used to determine the phase composition of the powder.

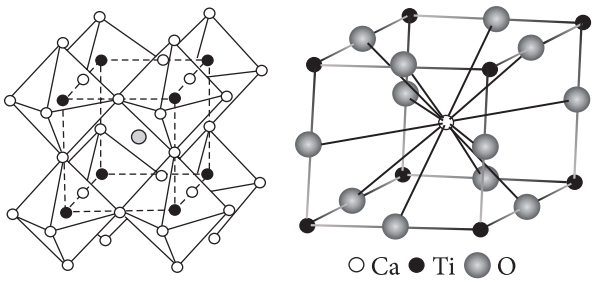

Fig. 1. The structure of perovskite $CaTiO_3$ [21]

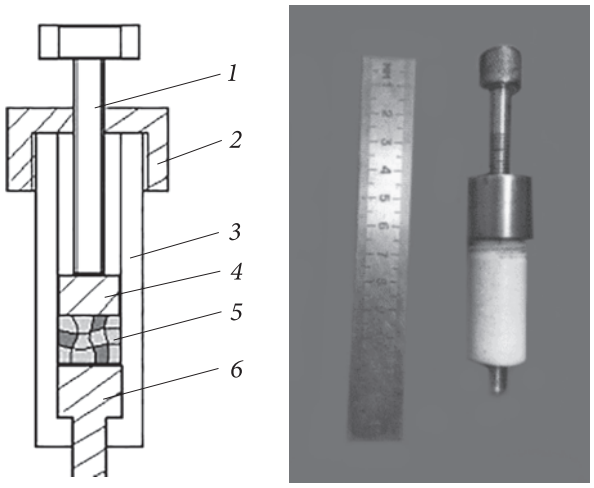

Fig. 2. Scheme of a two-electrode cell for measurement resistivity of the samples: *1* — screw; *2* — nut; *3* — teflon case; *4*, *6* — contact electrodes; *5* — test sample

The elemental composition of the initial powders was studied by X-ray fluorescence diffraction on XRD model Primini (Rigaku, Japan) using a palladium X-ray tube.

The resistivity of the sample was measured using a two-electrode cell (Fig. 2). Perovskite powder was ground in an agate mortar and pressed at a pressure of 200 MPa using alcohol moistening. The samples were sintered in a vacuum furnace (P = 10^{-2} Pa) at several temperatures for 1 hour, and then cooled together with the furnace. The samples were shaped as tablets with a diameter of 6.2 mm and a thickness of 4.52 mm. Their resistance was measured with an OWON XDM2041 digital multimeter. The resistivity (ρ) of the material was calculated using the equation:

$$\rho = S \times R/L,$$

where L is the tablet thickness; S is the tablet area; R is the cell resistance (measured with a multimeter).

Results of studies of perovskite samples and their discussion. Electronic density of states calculations for $CaTi_{1-x}Nb_xO_3$. The natural mineral perovskite rarely corresponds to the formula $CaTiO_3$ and often contains many impurities. For example, the isomorphic impurity of Nb in the form of Nb_2O_5 can reach [8] 26 wt.% (disanalyte). On the other hand, the use of special additives that replace one of the main elements in the $CaTiO_3$ lattice (doping) leads to alterations in the material's structural, electronic, optical, and other properties. The term "doping" is more commonly used in the field of developing materials for solar energy, thus it is used throughout this article. First principles calculations based on the density functional theory [13] make it possible to determine the theoretical values of the crystal lattice parameters, the positions of atoms in the unit cell, and the density of electronic states. By the location of the Fermi level, which separates the energy levels occupied by electrons from free levels, one can conclude whether the crystal is a dielectric (semiconductor) or a metal. In case of a dielectric (semiconductor), there is a band gap between the occupied and free states, which is absent in metals. In dielectrics, the width of the band gap is such that they have very low electrical conductivity at room temperature. The filled energy levels in semiconductors are also called the valence band, while the unfilled ones are called the conduction band. The calculation enables the determination of the width of the band gap and whether it is a direct or indirect band gap. To calculate the lattice parameters of doped crystals, the following two methods are used: the virtual crystal approximation (VCA) method [1] and the supercell method (SC — supercell) [11]. In the virtual crystal method, the potential within which the electrons are located is constructed as a superposition of the potentials of the initial atom and the dopant, each with their corresponding weight factors. This approach allows us to consider arbitrary dopant concentrations and requires computational efforts comparable to the calculation of pure crystals, since the symmetry of the original crystal is preserved. It is believed in the literature that the VCA method provides the most accurate results when the configurations of the valence electrons of the main atom and the dopant are identical, i.e. contain the same number of electrons in the outer s-, p-, d-orbitals. However, this method is also successfully used in other cases [18]. The SC method is based on increasing the size of the cell for which the calculation is performed. The elementary cell of the crystal repeats periodically in the directions of the main translation vectors of the crystal. This increases the volume of the cell and the number of atoms in it. Thus, a $2\times2\times1$ supercell for orthorhombic $CaTiO_3$ contains 80 atoms, out of which 16 are Ti atoms. By replacing one Ti atom with an Nb atom, we obtain a crystal with an Nb concentration of 1/16 = 6.25 at.%. To consider lower Nb concentrations, it is necessary to take a large supercell. Calculations involving cells with a large number of atoms demand significant computational time, along with the availability of large RAM and disk memory. This example highlights the limitations of the SC method, particularly its incapability to handle arbitrary and minor dopant concentrations.

Below are the results of calculations of the density of electronic states for niobium-doped $CaTiO_3$. When doped with niobium, niobium atoms replace titanium atoms [30]. The calculations were carried out using the Quantum Espresso software package [7] in the VCA approximation for niobium concentrations x = 0.03, 0.0625, 0.15, and 0.25. We used pseudopotentials from the library [26] with the GGA-PBE (Generalized Gradient Approximation) exchange-correlation potential [23]. Additionally, a calculation was performed for a niobium concentration of 0.0625 using a $2\times2\times1$ supercell.

In Figure 3 there are shown calculated densities of electronic states for $CaTiO_3$ doped with niobium. The vertical line indicates the position of the Fermi level, which divides the states occupied by electrons from the free states: states to the left of this level are occupied, while states to the right are free.

In pure $CaTiO_3$ (Fig. 3, *a*), the calculation indicates the existence of a band gap equals to 2.38 eV. This value is considerably lower than the experimental value characteristic of dielectrics, which is 3.7 eV [2]. This discrepancy is related to the fundamental property of the GGA-PBE exchange-correlation potential, which results in an inadequate estimation of the band gap in the electronic spectrum. However, for

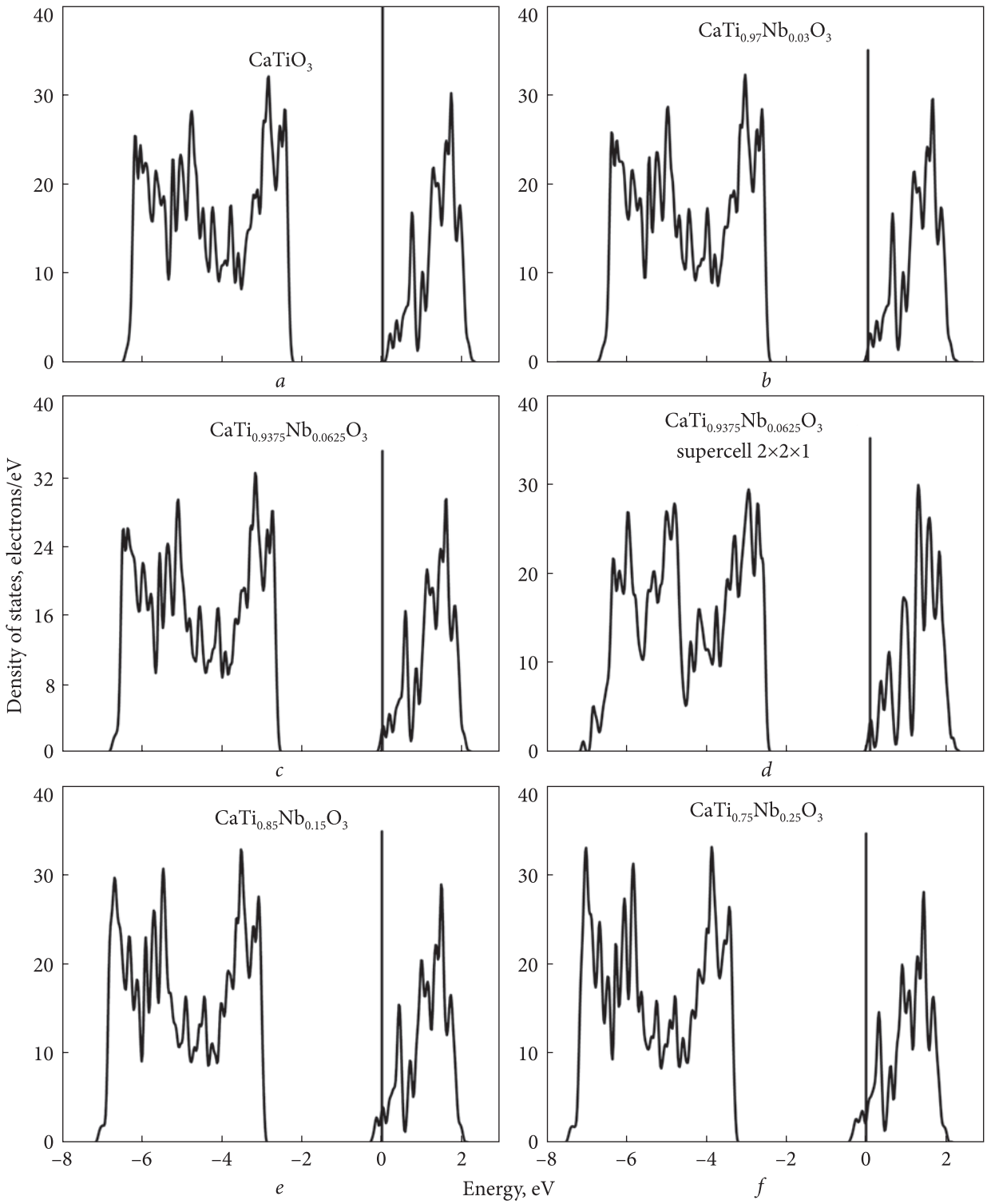

Fig. 3. Calculated densities of electronic states for $CaTi_{1-x}Nb_xO_3$: *a* — $x = 0.00$; *b* — $x = 0.03$; *c*, *d* — $x = 0.0625$; *e* — $x = 0.15$; *f* — $x = 0.25$

other physical quantities, such as lattice parameters and density of states, this potential shows good agreement with experimental data. For a niobium concentration of $x = 0.0625$, the density of states was calculated using both the VCA approximation and the $2 \times 2 \times 1$ supercell approximation — see Fig. 3, *c* and 3, *d*, respectively. A comparison of these figures shows agreement between the main characteristics of the density of states characteristics, including the number of

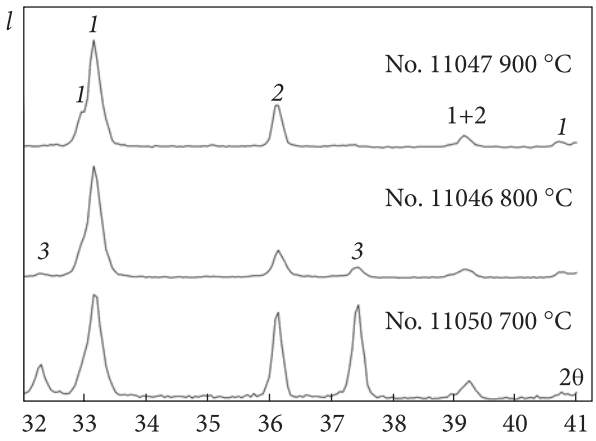

Fig. 4. XRD patterns showing the phase composition of pure perovskite samples depending on the synthesis temperature: *1* — $CaTiO_3$; *2* — TiO_2 (R); *3* — CaO

peaks, their relative positions, band widths, the gap width between the bands, and the position of the Fermi level. Thus, the use of the virtual crystal approximation is quite justified in this case.

From Figs. 3, *b*—*f*, it can be seen that there is practically no change in the general form of the density of states curves with an increase in niobium concentration. Since niobium has one more valence electron compared to titanium, as the niobium content increases, the Fermi level shifts to the band of free states. Such a shift in the Fermi level should lead to a change in the nature of the conductivity of doped crystals, eventually transitioning to metallic conductivity at high concentrations of niobium. However, for low concentrations of niobium, the number of electrons in the conduction band is small, and the transition to metallic state does not occur. Instead, we can observe conductivity with a value typical for semiconductors.

Thus, the performed studies have demonstrated the feasibility of using quantum mechanical calculations within the virtual crystal approximation to estimate the electronic properties of niobium-doped $CaTiO_3$. For low concentrations of niobium, the calculations indicate that the doped $CaTiO_3$ will exhibit conductivity characteristics typical of semiconductors.

Perovskite synthesis and X-ray studies of samples. For the synthesis of $CaTiO_3$ using the high-speed method, the initial charge of $Ti:Ca(OH)_2$ = 1:1 by mass ratio was used. Possible reactions during the heating of the initial mixture can be predicted as follows:

$$Ca(OH)_2 = CaO + H_2O \ (480\ °C)\ [9]$$

$$Ti + O_2 = TiO_2$$

$$TiO_2 + CaO = CaTiO_3$$

$$2Nb + 2.5O_2 = Nb_2O_5.$$

The synthesis time in the ceramic melting pot was 12 min. The results of qualitative and quantitative X-ray phase analysis of the obtained perovskite samples depending on the synthesis temperature are shown in Fig. 4 and Table 1.

At 700 °C (sample No. 11050), perovskite $CaTiO_3$ (~30% vol.) was obtained, although oxides CaO and TiO_2 are present in high quantities (Table 1). Consequently, the concentration of rutile is ~50% vol., and calcium oxide is ~19% vol. An increase in the synthesis temperature to 800 °C (sample No. 11046) led to an increase in the content of $CaTiO_3$ in the sample to 63% vol., while the rutile concentration decreased to 34% vol., and the CaO content

Table 1. **Phase composition of doped perovskite samples**

Phase		$CaTiO_3$	TiO_2 (rutile)	CaO	Nb_2O_5
No. sample	Temperature, °C	% vol.			
Samples without dopant					
11050	700	31	50	19	—
11046	800	63	34	3	—
11047	900	58	42	Traces	—
Samples with dopant					
11503	700	81	12	4	3
11507-11	800	76.5	14	5.5	4
11504	900	83	13	2.5	1.5

dropped to 3% vol. Subsequent elevation of the synthesis temperature to 900 °C caused a slight reduction in the concentration of $CaTiO_3$ to ~58% vol., accompanied by an increase in the content of TiO_2 to about 42% vol. It should be noted that, at this synthesis temperature, CaO is practically absent in the resulting powder.

For the synthesis of doped perovskite $CaTiO_3$ using the high-speed method, we used the initial load of $Ti:Ca(OH)_2:Nb = 1:1:0.3$ by mass ratio. The calculation showed that at the indicated ratios, up to 15% vol. Nb_2O_5 can form. The synthesis time in the ceramic melting pot was 5 min. Doping the perovskite results in the formation of a solid solution $Ca(Ti,Nb)O_3$. The results of qualitative and quantitative X-ray phase analysis of the obtained perovskite samples are shown in Fig. 5 and Table 1.

At a synthesis temperature of 700 °C (sample No. 11503), the content of $CaTiO_3$ is ~81% vol. Notably, TiO_2 is present in the powder at ~12% vol., CaO at about 4% vol., and Nb_2O_5 at approximately 3% vol. Increasing the synthesis temperature to 800 °C (sample No. 11507-11) leads to a slight decrease in the concentration of $CaTiO_3$ to ~76.5% vol. and a slight increase in the content of TiO_2 to ~14% vol., CaO to ~5.5% vol., and Nb_2O_5 to ~4% vol. in the sample. Subsequent temperature elevation to 900 °C results in an increase in the $CaTiO_3$ content to 83% vol., and a decrease in the concentrations of CaO to 2.5% vol. and Nb_2O_5 to 1.5% vol., while the content of TiO_2 remains almost unchanged (13% vol.).

The obtained results suggest that niobium significantly accelerates the synthesis reaction of

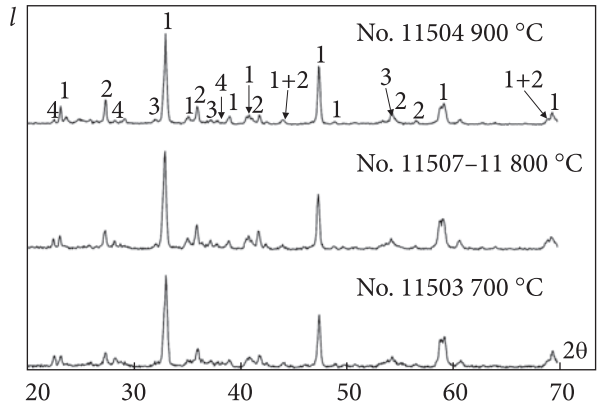

Fig. 5. XRD patterns showing the phase composition of doped perovskite samples depending on the synthesis temperature: *1* — $CaTiO_3$; *2* — TiO_2 (R); *3* — CaO; *4* — Nb_2O_5

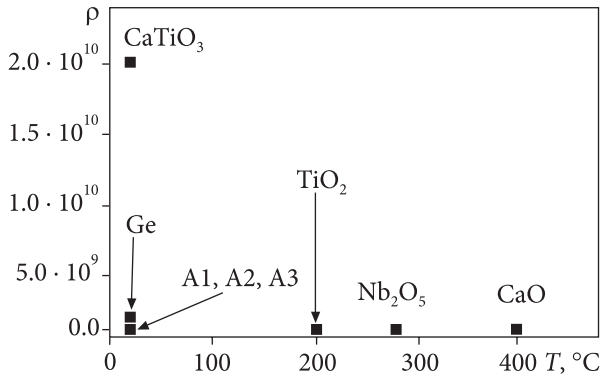

Fig. 6. Measured resistivity of synthetic samples A1, A2, and A3 in comparison with different materials (see Table 3)

Table 2. **Designation of samples and their sintering temperatures**

Sample	A1	A2	A3
Sintering temperature, °C	1000	1200	1400

Table 3. **Measured values of sample resistivity and literature data**

Compound	Temperature, °C	Resistivity, Ω·m	Reference
CaO	400	10^5	[15]
TiO_2	200	10^6	[15]
TiO_2(+Nb, Ta)	20	10^{-4}	[16]
Nb_2O_5	277	0.1	[15]
$CaTiO_3$	20	10^9	[10]
$CaTiO_3$	20	1.9×10^{10}	[27]
Ge	20	0.5	[14]
A1	20	0.708	—
A2	20	0.0071 (with paste)	—
A3	20	0.0018 (with paste)	—

$CaTiO_3$. At a temperature of 900 °C, with a synthesis time of 5 min, the presence of niobium results in a concentration of 83% perovskite $CaTiO_3$ in the sample. In contrast, using a mixture without Nb, the content of perovskite is only 58% when synthesized for 12 min. Furthermore, a significant decrease in the concentration of Nb_2O_5 compared to the calculated value, along with the absence of other niobium-based phases, indicates the formation of a Ca(Ti,Nb)O_3 solid solution, which can lead to significant changes in the properties of perovskite. With an increase in the synthesis temperature to 900 °C, the content of niobium oxide decreases (to 1.5% vol.) and, consequently, the content of Nb in the Ca(Ti,Nb)O_3 lattice increases.

Investigation of the resistivity of doped $CaTiO_3$. In its pure perovskite form, $CaTiO_3$ is a dielectric, which is confirmed by resistivity measurements (ρ). The specific resistance of $CaTiO_3$ at 20 °C was 10^{10} Ω·m [10], results from measurements of ρ at the same temperature in [27] showed a value of $1.9 \cdot 10^{10}$ Ω·m. It should also be noted that according to [16], pure rutile crystals of TiO_2 has a resistivity ρ = 10^4—10^6 Ω·m, which is lowered to ρ = 10^{-4} Ω·m by niobium and tantalum impurities. The resistivity value (ρ) of CaO changes from 10^5 to 10^2 Ω·m within the temperature range of 400 °C to 1000 °C [15].

Literary data, along with first principles calculations, indicate that one possible method for obtaining highly efficient solar cells based on $CaTiO_3$ could involve doping it with niobium. One outcome of this doping will be a decrease in resistivity to values more typical for semiconductors. According to [16], the resistivity of semiconductors is:

$$\rho = 10^{-6}—10^{8}\ \Omega \cdot m.$$

Summarizing mentioned above, the resistivity of samples derived from niobium-doped perovskite, obtained by high-speed synthesis, was measured. The studies were carried out according to the procedure and equipment described earlier. The synthesized perovskite powder samples were sintered at appropriate temperatures (Table 2). The outcomes of resistivity measurements for the samples, along with literary data, are presented in Table 3 and Fig. 6.

The results given in Table 3 and Fig. 6 show that the resistivity of pure perovskite $CaTiO_3$ is 10^9—10^{10} Ω·m, as is inherent for a dielectric material. The results of the study indicate that during the rapid synthesis of perovskite samples using the Nb dopant, the resistivity value significantly decreases, whereas the resistivity of the composite ($CaTiO_3$ + TiO_2) is approximately 10^{-3} Ω·m. That is, the resistivity of composite samples ($CaTiO_3$ + TiO_2) approaches the values inherent for semiconductors.

Conclusions. 1. The calculation of electronic states density for niobium-doped $CaTiO_3$ has shown that at low concentrations of niobium, conductivity characteristics typical of semiconductors are observed.

2. Fundamental principles for the high-speed synthesis of doped perovskites with semiconductor properties have been developed.

3. X-ray phase analysis of the composite ($CaTiO_3$ + TiO_2) showed that the use of niobium as a doping element significantly accelerates the $CaTiO_3$ synthesis reaction, while increasing the perovskite concentration in the system.

4. X-ray phase analysis of the composite revealed the formation of a solid solution of Ca(Ti, Nb)O_3, resulting in the production of composite samples ($CaTiO_3$ + TiO_2) with resistivity values approaching those inherent to semiconductors.

5. The study of high-speed synthesis of the composite within 3—12 minutes in the temperature range of 700—900 °C enables the development of energy-saving laboratory and industrial technologies for producing $CaTiO_3$ perovskite powder, which can be utilized in semiconductor ceramics.

REFERENCES

1. Bellaiche, L. and Vanderbilt, D. (2000), *Phys. Rev. B,* Vol. 61, Iss. 12, pp. 7877-7882. https://doi.org/10.1103/PhysRevB.61.7877
2. Boutinaud, P., Pinel, E., Dubois, M., Vink, A.P. and Mahiou, R. (2005), *J. Lumin.,* Vol. 111, Iss. 1-2, pp. 69-80. https://doi.org/10.1016/j.jlumin.2004.06.006
3. Cheng, Z. and Lin, J. (2010), *CrystEngComm.,* Vol. 12, pp. 2646-2662. https://doi.org/10.1039/C001929A

4. Council, UNDP; UN. WE Energy and the challenge of sustainability, 2000. New York, UNDP, 2000.
5. Ehsan, M. Ali, Naeem, R., McKee, V., Rehman, A., Hakeem A.S. and Mazhar, M. (2019), *J. Mater. Sci.: Mater. Electron.,* Vol. 30, pp. 1411-1424. https://doi.org/10.1007/s10854-018-0411-4
6. (2018) *Enerdata Global Energy Statistical Yearbook* 2018. URL: https://yearbook.enerdata.net/total-energy/world-consumption-statistics.html (Accessed: Septem. 2018).
7. Giannozzi, P., Baroni, S., Bonini, N., Calandra, M., Car, R., Cavazzoni, C., Ceresoli, D., Chiarotti, G.L., Cococcioni, M., Dabo, I., Corso, A.D., Gironcoli, S., Fabris, S., Fratesi, G., Gebauer, R., Gerstmann, U., Gougoussis, C., Kokalj, A., Lazzeri, M., Martin-Samos, L., Marzari, N., Mauri, F., Mazzarello, R., Paolini, S., Pasquarello, A., Paulatto, L., Sbraccia, C., Scandolo, S., Sclauzero, G., Seitsonen, A.P., Smogunov, A., Umari, P. and Wentzcovitch, R.M. (2009), *J. Phys.: Cond. Matter*., Vol. 21, No. 39, 395502 (19 p.). https://doi.org/10.1088/0953-8984/21/39/395502
8. Godovikov, A.A. (1975), *Mineralogy*, Nedra, Moscow, 520 p. [in Russian].
9. Goronovsky, I.T., Nazarenko, Yu.P. and Nekryach, E.F. (1974), *Quick guide to chemistry,* Nauk. dumka, Kyiv, 992 p. [in Russian].
10. Gralik, G., Thomsen, A.E., Moraes, C.A., Raupp-Pereira, F. and Hotza, D. (2014), *Processing and Application of Ceramics,* Vol. 8, No. 2, pp. 53-57. https://doi.org/10.2298/PAC1402053G
11. Haksung, L., Teruyasu, M., Takahisa, Y. and Yuichi, I. (2009), *Materials Transactions,* Vol. 50, Iss. 5, pp. 977-983. https://doi.org/10.2320/matertrans.MC200813
12. Han, C., Liu, J., Yang, W., Wu, Q., Yang, H., Xue, X. and Sol-Gel, J. (2016), *Sci. Technol.*, Vol. 81, pp. 806-813. https://doi.org/10.1007/s10971-016-4261-3
13. Hohenberg, P. and Kohn, W. (1964), *Phys. Rev.,* Vol. 136, Iss. 3B, pp. 864-871. https://doi.org/10.1103/PhysRev.136.B864
14. Knunyants, I.L. and Zephirov, N.S. (ch. ed.) (1988), *Chemical encyclopedia,* Vol. 1, Soviet Encyclopedia Publ. House, Moscow, 623 p. [in Russian].
15. Krzhizhanovsky, R.E. and Stern, Z.Yu. (1973), *Thermophysical properties of non-metallic materials (Oxides),* Energia publ., Leningrad, 336 p. [in Russian].
16. Kulikov, B.F., Zuev, V.V., Vainshenker, I.A. and Mitenkov, G.A. (1985), *Mineralogical handbook of the enrichment technologist,* Nedra, Leningrad, 264 p. [in Russian].
17. Li, S., Li, X., Yang, J., Jiang, Q., Lai, H., Tan, Y., Xiao, B. and Xu, T. (2020), *J. Power Sources,* Vol. 449, 227504. https://doi.org/10.1016/j.jpowsour.2019.227504
18. Liao, M., Liu, Y. and Mina, L. (2018), *Intermetallics,* Vol. 101, pp. 152-164. https://doi.org/10.1016/j.intermet.2018.08.003
19. Liu, G., Yang, B., Chen, H., Zhao, Y., Xie, H., Yuan, Y., Gao, Y. and Zhou, C. (2019), *Appl. Phys. Lett.,* Vol. 115, pp. 213501-1-213501-5. https://doi.org/10.1063/1.5131300
20. Lozano-Sánchez, L.M., Lee, Soo-Wohn, Sekino, Tohoru and Rodríguez-González, V. (2013), *CrystEngComm.,* Vol. 15, pp. 2359-2362. https://doi.org/10.1039/C3CE27040H
21. Pavlishin, V.I. and Dovgy, S.O. (2008), *Mineralogy,* Pidruchnyk, KMT publ., Kyiv, 536 p. [in Ukrainian].
22. Pavlyshyn, V.I., Voroshylov, Yu.V. and Kvasnytsya, I.V. (2017), *Mineralogy,* Pidruchnik, VPC Kyiv, Univ. publ., Kyiv, 528 p. [in Ukrainian].
23. Perdew, J., Burke, K. and Ernzerhof, M. (1996), *Phys. Rev. Lett.,* Vol. 77, Iss. 18, pp. 3865-3868. https://doi.org/10.1103/PhysRevLett.77.3865
24. Pereira, S., Figueiredo, A., Barrado, C., Stoppa, M. and Dwivedi, Y. (2015), *J. Braz. Chem. Soc.,* Vol. 26, No. 11, pp. 2339-2345. https://doi.org/10.5935/0103-5053.20150229
25. Ponomarenko, O.M., Smolyar, A.S., Burkhan, A.O., Maloshtan, S.M., Bloshchanevich, O.M., Stegniy, A.I., Khomenko, B.S. and Titenko, A.M. (2020), *Abstracts Int. sci. conf. "Materials for work in extreme conditions — 10" (Dec. 10-11, 2020, Kyiv,* Igor Sikorsky Nat. Techn. Univ. "KPI"), IMZ named Ye.O. Paton, Kyiv, pp. 64-66 [in Ukrainian].
26. (2022) *Quantum Espresso website.* URL: http: www.quantum-espresso. org/pseudopotentials (Accessed: April. 2022).
27. Rocha-Rangel, E., López-Hernández, J., Castello-Martínez, J., Osorio-Ramos, J.J., Calles-Arriaga, C.A., Estrada-Guel, I. and Martínez-Sánchez, R. (2018), *Arch. Metall. Mater.,* Vol. 63, No. 4, pp. 1749-1753. https://doi.org/10.24425/amm.2018.125101
28. Smolyar, A.S., Burkhan, A.O., Bloshchanevich, O.M., Stegniy, A.I., Stepanenko, A.V., Brodnikovsky, M.P. and Titenko, A.M. (2022), *Abstracts Int. sci. conf. "Materials for work in extreme conditions — 12" (Dec. 15, 2022, Kyiv,* Igor Sikorsky Nat. Techn. Univ. "KPI"), IMZ named Ye.O. Paton, Kyiv, pp. 31-32 [in Ukrainian].
29. Smolyar, A.S., Burkhan, A.O., Ponomarenko, O.M., Maloshtan, S.M., Khomenko, B.S. and Titenko, A.M. (2019), *Abstracts Int. sci. conf. "Materials for work in extreme conditions — 9" (Dec. 18-19, 2019, Kyiv,* NTUU "KPI named after Igor Sikorsky"), Kyiv, 2019, pp. 10-13 [in Ukrainian].
30. Ueda, K., Yanagi, H., Hosono, H., and Kawazoe, H. (1997), *Phys. Rev. B*, Vol. 56, Iss. 20, pp. 1298-13005. https://doi.org/10.1103/PhysRevB.56.12998
31. Voroshilov, Yu.V. and Pavlishin, V.I. (2011), *Fundamentals of crystallography and crystal chemistry. X-ray diffraction of crystals,* KNT publ., Kyiv, 568 p. [in Russian].

32. Yang, H., Han, C. and Xue, X. (2014), *J. Environ. Sci.,* Vol. 26, No. 7, pp. 1489-1495. https://doi.org/10.1016/j.jes.2014.05.015
33. Zeng Pu-jun, Yu Li-ping, Qiu Zhong-xian, Zhang Ji-lin, Rong Chun-ying, Li Cheng-zhi, Fu Zai-hui and Lian Shi-xun (2012), *J. Sol. Gel. Sci. Technol.*, Vol. 64, pp. 315-323. https://doi.org/10.1007/s10971-012-2860-1
34. Zhang, X., Zhang, J., Ren, X. and Wang, X. (2008), *J. Solid State Chemistry,* Vol. 181, No. 3, pp. 393-398. https://doi.org/10.1016/j.jssc.2007.11.022
35. Zhao, H., Duan, Y. and Sun, X. (2013), *New J. Chem.,* Vol. 37, pp. 986-991. https://doi.org/10.1039/C3NJ40974K

Received 28.04.2023

О.М. Пономаренко[1], д-р геол. наук, акад. НАН України, директор
E-mail: pan.igmof@gmail.com; https://orcid.org/0000-0002-5179-6091
Л.М. Степанюк[1], д-р геол. наук, чл.-кор. НАН України, проф., заст. дир.
E-mail: stepaniuk@nas.gov.ua; https://orcid.org/0000-0001-5591-5169
А.С. Смоляр[1], канд. техн. наук, старш. наук. співроб.
E-mail: smolyar@nas.gov.ua; https://orcid.org/0009-0002-2201-6823
А.О. Бурхан[1], канд. техн. наук, старш. наук. співроб.
E-mail: burhan.anatoliy@ukr.net; https://orcid.org/0009-0002-3155-0171
О.М. Блощаневич[2], наук. співроб.
E-mail: alex.bl337777@gmail.com; https://orcid.org/0009-0008-3624-9082
А.І. Стегній[2], наук. співроб.
E-mail: steg888999@gmail.com; https://orcid.org/0009-0007-4082-4425
В.Л. Бекеньов[2], старш. наук. співроб.
E-mail: alitub@ukr.net; https://orcid.org/0009-0003-2438-4731
А.В. Степаненко[1,2], канд. фіз.-мат. наук, старш. наук. співроб.
E-mail: stepart6913@gmail.com; https://orcid.org/0000-0003-2282-146X
В.Г. Хоменко[3], д-р техн. наук, доцент
E-mail: v.khomenko@i.ua; https://orcid.org/0000-0003-0013-8010
М.П. Бродніковський[2], канд. фіз.-мат. наук, зав. відділу
E-mail: nbrodnik@gmail.com; https://orcid.org/0000-0001-7649-7373
Б.С. Хоменко[4], пров. інженер
E-mail: bskhomenko40@gmail.com; https://orcid.org/0009-0006-0707-7707
[1] Інститут геохімії, мінералогії та рудоутворення ім. М.П. Семененка НАН України
03142, м. Київ, Україна, просп. Акад. Палладіна, 34
[2] Інститут проблем матеріалознавства ім. І.М. Францевича НАН України
03142, м. Київ, Україна, вул. Омеляна Пріцака, 3
[3] Київський національний університет технологій та дизайну
01011, м. Київ, Україна, вул. Мала Шияновська, 2
[4] Інститут загальної та неорганічної хімії ім. В.І. Вернадського НАН України
03142, м. Київ, Україна, просп. Акад. Палладіна, 32/34

ГУСТИНА ЕЛЕКТРОННИХ СТАНІВ, ПИТОМИЙ ОПІР І ФАЗОВИЙ СКЛАД ПЕРОВСЬКІТУ $CaTiO_3$ З ІЗОМОРФНОЮ ДОМІШКОЮ НІОБІЮ

Застосування матеріалів зі структурою перовськіту сьогодні стало одним із найперспективніших підходів до розробки фотоелектричних систем. Розроблено методику високошвидкісного (до 15 хв) синтезу композиту (перовськіт $CaTiO_3$ + рутил TiO_2) з можливістю одночасного допування продукту. Досліджено щільність електронних станів легованого ніобієм перовськіту ($CaTiO_3$), особливості фазового складу та питомий опір композиту ($CaTiO_3$ + TiO_2). Розрахунки електронних станів густини $CaTiO_3$, допованого ніобієм, показали, що за низької концентрації Nb зразки демонструють провідність, характерну для напівпровідників. Оскільки ніобій має на один валентний електрон більше ніж титан, то зі збільшенням його вмісту рівень Фермі зсувається в зону вільних станів. Такий зсув рівня Фермі повинен спричинити зміни характеру провідності допованих кристалів аж до переходу до металевої провідності за високої концентрації ніобію. Аналіз композиту ($CaTiO_3$ + TiO_2) методом рентгенівської дифракції показав, що використання ніобію як елемента допування значно прискорює реакцію синтезу $CaTiO_3$ і підвищує концентрацію перовськіту в зразку: за температури 900 °C протягом 5 хв синтезу концентрація $CaTiO_3$ у зразку з ніобієм становить 83 % об., а у разі використання суміші без Nb вміст перовськіту становитиме лише 58 % об. за 12 хв. Методами рентгенофазового аналізу встановлено, що у випадку утворення твердого розчину (допування) виникає $Ca(Ti,Nb)O_3$, у результаті чого можна отримати зразки ($CaTiO_3$ + TiO_2) з питомим опором, властивим напівпровідникам.

Ключові слова: перовськіт, синтез, рентгенівські дослідження, допування, напівпровідник, провідність.